Automotive Science and Engineering, Vol. 15, No. 2, (2025), 4739-4754

Iran University of Science and Technology

Automotive Science and Engineering

Journal Homepage: ase.iust.ac.ir

ISSN: 2008-9899

A Novel Parallel Control Architecture for Integrated Electro-Hydraulic Brake to Simultaneously Enhance Braking Performance and Vehicle Stability

Nayereh Raesian [1*], Hossein Gholizadeh Narm [2]

[1] Shahrood University of Technology

[2] Shahrood University of Technology

ARTICLE INFO

Article history:

Received: 24 Feb 2025

Accepted: 25 May 2025

Published: 15 June 2025

Keywords:

Electro-hydraulic brake system control

Electronic stability control

Differential braking

Integrated control

Emergency braking

A B S T R A C T

Emergency braking during cornering is one of the main challenges in vehicle dynamics. This paper proposes a novel parallel control architecture for Electro-Hydraulic Braking (EHB) systems that dynamically balances the priorities of Emergency Braking (EB) and Electronic Stability Control (ESC) using a fuzzy-GA optimizer. . The proposed approach achieves significant improvements in yaw stability without compromising deceleration performance. The proposed control structure consists of two parallel branches that adjust the required pressure for each wheel and uses two inputs: the steering angle and the position of the driver's foot on the brake pedal. The control system is structured in such a way that it simultaneously calculates the vehicle deviation value using the sliding mode controller and then determines the appropriate pressure to compensate for this deviation, while at the same time estimating the appropriate brake pressure based on the brake pedal input. To effectively apply these inputs to the vehicle braking system this paper introduces an innovative approach that uses a fuzzy controller optimized through a genetic algorithm.

1. Introduction

Braking while cornering, especially if it is an emergency brake, can challenge the control of the Electronic Stability Control (ESC) system due to the combination of lateral (steering) and longitudinal (braking) forces. Emergency braking on a straight road may also lead to a disruption of vehicle stability control under certain conditions, although this is less likely than when cornering. Such disruptions usually result from improper distribution of brake force due to uncoordinated interactions between the braking and stability control systems. In addition, activating the stability control system can reduce the effectiveness of emergency braking during cornering and increase deceleration time. This paper presents an integrated and parallel architecture for effective control of wheel brake pressure when both ESC and emergency braking are in use. By monitoring the steering angle and pedal travel inputs from the driver, the challenge of maintaining vehicle stability while ensuring timely deceleration is overcome. In addition, the Anti-lock Braking System (ABS) control system in this framework helps to prevent wheel lockup.

The Electro-Hydraulic Brake (EHB) System is an innovative electronic braking solution (Brake-by-Wire) that replaces the traditional vacuum booster, integrating multiple functions to advance

*Corresponding Author
Email Address: n.raesian@shahroodut.ac.ir
https://doi.org/10.22068/ase.2025.708

[DOI: 10.22068/ase.2025.708]

intelligent vehicle technologies. This system consolidates key technologies such as vehicle stability control, anti-lock braking, traction control, and regenerative braking, all seamlessly unified within the electronic braking framework. The EHB system primarily comprises two main components: a servo motor unit and a hydraulic control unit. The permanent magnet synchronous motor (PMSM) generates high, stable pressure in the master cylinder, while the four-channel hydraulic control unit ensures precise and independent pressure modulation for each wheel cylinder [1-3].

Recent research has explored various control methods to optimize PMSM performance. One approach involves using a fuzzy logic controller with direct torque control, shown to enhance PMSM performance characteristics [4]. Vector control techniques have also gained traction, particularly for synchronous motor control, where a Neural Network (NN)-based vector controller demonstrates robust, adaptive performance in dynamic conditions [5],[6]. Additionally, the Direct Torque Control (DTC) method, widely utilized for electric motor control, has seen advancements through Space Vector Modulation (SVM-DTC) for improved modulation precision and responsiveness [7]. Advanced control techniques, such as Model Predictive Control (MPC), offer significant advantages by directly tuning controllers and managing constraints effectively. To address the computational demands associated with extended prediction horizons, Nonlinear Model Predictive Control (NMPC) has been introduced as a refined approach suitable for real-time applications, providing precision with a shorter prediction horizon [8],[9]. Model Predictive Torque Control (MPTC) further improves system performance, enabling rapid response and efficient real-time operation [10].

Several robust control techniques have also been developed for PMSM regulation, including methods that ensure stability across nonlinear electric dynamics [11]. Sliding Mode Control (SMC), coupled with low-pass filtering, effectively compensates for system uncertainties, while combining Sliding Mode Variable Structure Control (SMVSC) with fuzzy logic introduces a hybrid approach that leverages the strengths of both methods [12],[13]. Recently, Continuous Fast Terminal Sliding Mode Control (CFTSMC) has been employed for high-precision speed regulation in PMSMs [14].

Position tracking in electronic brake boosters remains a significant challenge due to the system's highly nonlinear characteristics and load-dependent friction. A proposed solution is a three-loop PI position tracking control structure [15]. Research in this area has also suggested an advanced control strategy using Maximum Torque per Ampere (MTPA) with adaptive current weakening for rapid response and precise position tracking [16]. Another notable approach includes a nonlinear control method for auxiliary braking, incorporating signal processing, driver brake behavior detection, and precise position control for the PMSM [17].

Accurate pressure control relative to the master cylinder's shaft positions is crucial for EHB systems. To this end, several adaptive controllers have been proposed. One adaptive sliding-mode hydraulic pressure controller, relying on a hydraulic pressure estimator, aims to achieve sensor less tracking of the desired pressure [18]. Another study developed a robust adaptive controller to enhance pressure tracking using a continuous friction model [19]. Additionally, Fuzzy-PI and Fuzzy control methods have been employed to regulate the EHB system's hydraulic pressure cylinder [20],[21]. An adaptive controller integrating fuzzy logic to dynamically adjust the weighting of a Linear Quadratic Regulator (LQR) has also been explored [22]. Furthermore, a feed-forward control law for pressure tracking aims to enhance response speed by controlling the main piston rod's position in the cylinder [23].

Incorporating dynamic vehicle stability control in EHB systems is another promising direction, with recent research highlighting hierarchical control architectures. For instance, variable structure sliding-mode controllers within hierarchical frameworks have shown potential in enhancing vehicle stability [1]. A cascade controller based on a nonlinear observer was also developed for cylinder pressure tracking, effectively handling external disturbances and parameter uncertainties

[DOI: 10.22068/ase.2025.708]

[23]. A three-layered stability control structure has been proposed to address dynamic vehicle instability, consisting of decision-making, distribution, and execution layers based on EHB systems [24].Recently, in a paper, a H∞ controller is used correctly to control the vehicle roll angle, and good results have been obtained [25]. Hierarchical control on ESC has also recently gained interest among researchers [26].

In recent years, integrated systems with differential braking have been increasingly studied to improve vehicle stability. These systems leverage differential braking alongside other technologies, such as active steering and active aerodynamic control, for enhanced stability management [27],[28].

The use of genetic algorithms in control optimization has garnered attention in recent years. Recently, it has been implemented in a study on fuzzy and PID controllers, fuzzy sliding mode controller, aiming to examine the influence of two controllers in an active seat suspension system for enhancing ride comfort in a semi-trailer truck [29],[30].

The present paper proposes a parallel structure for stability control and emergency braking. The particular focus in this paper is to analyze emergency braking in curves, ensuring that at all times vehicle steering ability and the desired speed of deceleration and braking by the driver are preserved. A fuzzy control system can detect curve emergency braking and decide in each moment whether the priority is vehicle stability or deceleration and braking. Therefore, the system transmits the desired maximum pressure within the distribution system to apply a desired pressure on each wheel based on the appropriate distribution algorithm until the emergency brake and deviation conditions for the resolution are achieved.

Thus, on a straight road without any noticeable vehicle deviation, when emergency braking or normal braking is applied, the application is made using emergency or standard pressure distribution algorithms within EHB (Electronic Hydraulic Brakes) with accurate pressure control. The fuzzy control system is not operational at this stage. Similarly, when stability control is the only requirement, and emergency braking has not been detected, the fuzzy control system remains inactive, and the desired pressure is computed and applied per the distribution algorithm displayed in fig. 7.In all these scenarios, if the pressure applied to the wheels leads to their locking, the ABS control system intervenes to prevent the wheels from locking.

In the present study, first, the proposed control system architecture is given; and simulation result and analysis are offered. Finally, the conclusion is studied.

2. Proposed control system architecture

The control architecture features two parallel control systems, as illustrated in fig. 1. The stability controller on the right employs a hierarchical structure to enhance performance and stability. It computes the corrective yaw moment for dynamic tracking using a sliding mode controller that processes the driver's steering angle input, integrates it with the vehicle's dynamic model, and determines the desired yaw rate and slip angle. Concurrently, the schematic on the left incorporates the driver’s pedal movement into the dynamic model of the Electro-Hydraulic Brake (EHB) to ascertain the necessary brake system pressure. Additionally, in this section, the emergency brake is identified based on the pedal pressing speed (Pedaling speed above 7 mm/s).

The pressures derived from both systems are processed by a fuzzy controller optimized via a genetic algorithm, which calculates the appropriate pressure coefficients for wheel application during braking. This controller activates only when both the Emergency braking (EB) and the Electronic Stability Control (ESC) system are engaged; otherwise, the calculated pressures are applied directly. The EHB control section employs a cascade controller with two closed loops: an outer loop for cylinder pressure control and an inner loop for rack position control, aimed at regulating external pressure through a desired position signal for the internal controller.

The lower parts of the braking system are critical for coordinating the differential brakes to maintain

[DOI: 10.22068/ase.2025.708]

optimal pressure distribution at the wheels. These components are essential to ensure vehicle stability, prevent wheel lock and timely braking by accurately regulating the brake pressure applied to each wheel. An anti-lock braking system (ABS) controller monitors this complex process and uses a self-tuning PID controller with an adaptive neuro-fuzzy inference system (ANFIS).This integration enhances the system's responsiveness and adaptability under varying driving conditions.

In the following sections, we will provide a detailed examination of each component that comprises this control structure.

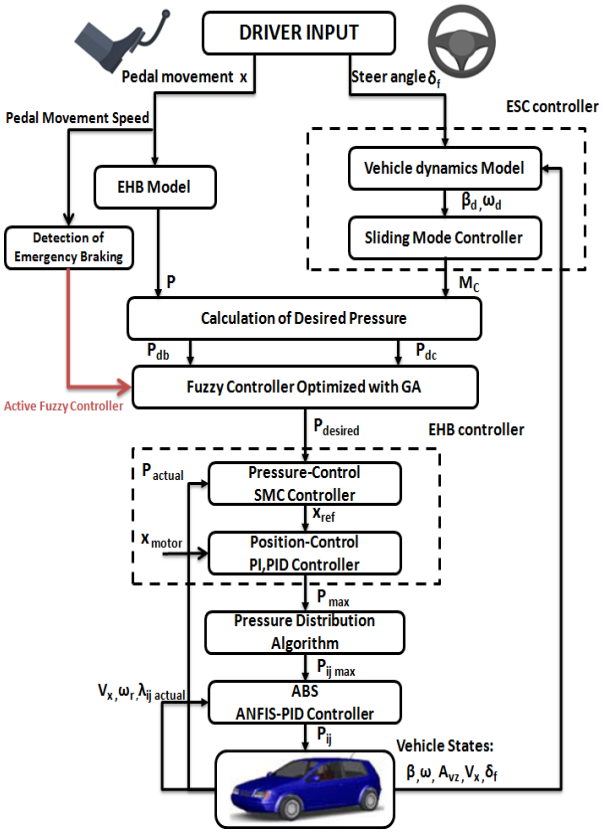

Figure 1. Proposed control system architecture

2.1. Control Vehicle Stability

In this section, we calculate the necessary correction pressure for the differential braking of the wheels based on the degree of deviation of the vehicle from the driver's steering angle input.

2.1.1. Vehicle Dynamic Model

Fig.2 shows the four-wheel model of the car, in which the front wheels were labeled as *f* and the back wheels as *r*. The right and left edges of the car are represented by *R* and *L*. The center of gravity is represented by the symbol *C.G.*, while the distance from the center of gravity to the axle is labeled as *a*, and as the back the axle is as *b*. The total length from the back of the car is indicated by *L*.

By assuming that both front and rear wheels are paired together and taking the center of gravity as the origin of the coordinate system. In this model, $\omega_r$represents the yaw rate, u denotes the longitudinal velocity, and v the lateral velocity. The complete model includes all motion and physical details of the vehicle, such as the effects of each component, the relationships between parts, and the forces acting on the vehicle. This results in much more precise and realistic stability analysis [31]. However, in many cases, the full vehicle model is highly complex; therefore, using a two-degree-of-freedom model is an effective way to analyze stability and determine the need for appropriate auxiliary torque. It allows for rapid and reasonably accurate estimation of the effects of auxiliary torque by focusing on two key variables, such as the yaw angle and lateral movement. Additionally, models with fewer degrees of freedom require simpler calculations, which is important in the design of controllers and active driver assistance systems where fast decision-making is crucial. So, this section is based on the two-degree-of-freedom (2-DOF) vehicle model, which serves as the reference model for the car's dynamics.

If we express Newton's laws for this model, we have:

$$\sum F_y = ma_y \tag{1}$$

where *m* is the mass of the vehicle, and a_y is the acceleration of the vehicle in the Y-axis direction, determined by the following equation:

$$a_y = \dot{v} + u\omega_r \tag{2}$$

In the two degrees of freedom vehicle model, F_{yf} and F_{yr} represent the lateral forces on the front and rear tires, respectively. In fig.2, the moment of inertia around the Z-axis is denoted as I_z, and $\dot{\omega}_r$ represents the angular acceleration. By expanding and combining the aforementioned formulas, we obtain:

$$F_{yf} + F_{yr} = m(\dot{v} + u\omega_r) \tag{3}$$

$$aF_{yf} - bF_{yr} + M_c = I_z\,\dot{\omega}_r \tag{4}$$

[DOI: 10.22068/ase.2025.708]

M_c represents the corrective torque, which is the amount of torque applied to the vehicle to keep it on the desired path. If the vehicle is steered at an angle δ , we observe that the vehicle moves in the direction of a smaller angle. The difference between the steering angle δ and this angle is referred to as the tire slip angle α. The forces acting on the tires within the linear range can be expressed as follows, with coefficients α_f for the front tires and α_r for the rear tires. Additionally, β represents the vehicle's slip angle, as shown in Fig. 2 [27].

$$\alpha_f = \beta + \frac{a\omega_r}{u} - \delta \tag{5}$$

$$\alpha_r = \beta - \frac{b\omega_r}{u} \tag{6}$$

For small slip angles, the tire's lateral force is directly proportional to the slip angle. This assumption can provide acceptable results in normal and reduced extreme maneuvers, but may be flawed when dealing with extreme, nonlinear maneuvers such as changes in tire stiffness.

$$F_{yf} = C_f\alpha_f \tag{7}$$

$$F_{yr} = C_r\alpha_r \tag{8}$$

C_f=80000 N/rad ±5% due to tire wear and C_r = 50000 N/rad ±4% due to temperature effects, denote the lateral stiffness values for the front and rear tires, respectively.

By arranging these equations as a system and simplifying them, the vehicle dynamic state-space equations can be derived as follows:

$$\dot{\beta} = \frac{C_f + C_r}{mu}\beta + \left(\frac{aC_f - bC_r}{mu^2} - 1\right)\omega_r \tag{9}$$

$$\dot{\omega}_r = \frac{aC_f - bC_r}{I_z}\beta + \frac{a^2C_f + b^2C_r}{I_z u}\omega_r - \frac{aC_f}{I_z}\delta \tag{10}$$

The goal of this controller is to ensure the vehicle's stability. This component utilizes various internal sensor measurements, calculating the desired vehicle dynamics and corrective torque for stability control. Thus, the desired yaw rate ω_d and lateral slip angle β_d for the vehicle can be determined from the steering angle, vehicle speed, road-tire friction coefficient, and vehicle parameters as following [32]:

$$\omega_d = \min\left(\left|\frac{u/l}{1 + \frac{mu^2(aC_f - bC_r)}{L^2C_fC_r}}\delta\right|, \left|\frac{0.85\mu}{u}\right|\right) \times \operatorname{sgn}\left(\frac{u/l}{1 + \frac{mu^2(aC_f - bC_r)}{L^2C_fC_r}}\delta\right) \tag{11}$$

$$\beta_d = \min\left(\left|\left(\frac{b}{L(1 + Ku^2)} + \frac{mau^2}{C_rL^2(1 + Ku^2)}\right)\delta\right| \times \operatorname{sgn}\left(\left(\frac{b}{L(1 + Ku^2)} + \frac{mau^2}{C_rL^2(1 + Ku^2)}\right)\delta\right)\right) \tag{12}$$

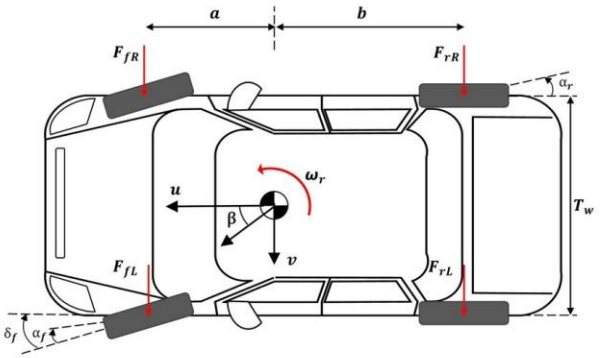

Figure 2. The vehicle model

2.1.2. Direct Yaw Moment Control

Electronic Stability Control (ESC) is a fundamental technology for stabilizing two-dimensional vehicle motion, and Direct Yaw Moment Control (DYC) is a practical and effective approach for implementing ESC. In this study, a sliding mode controller is developed to calculate the corrective torque (M_c). The sliding surface is defined as follows [28]:

$$s = \omega_r - \omega_d + \zeta(\beta - \beta_d) \tag{13}$$

Taking the derivative of the above equation:

$$\dot{s} = \dot{\omega}_r - \dot{\omega}_d + \zeta\left(\dot{\beta} - \dot{\beta}_d\right) \tag{14}$$

As noted in [33]:

$$\frac{1}{2}\frac{d}{dt}s^2 = s\dot{s} \le -\eta s^2 \tag{15}$$

[DOI: 10.22068/ase.2025.708]

$$M_c = I_z\big(\dot{\omega}_d - \eta\big(\omega_r - \omega_d + \zeta(\beta - \beta_d)\big) - \zeta(\dot{\beta} - \dot{\beta}_d)\big) - (aC_f - bC_r)\beta + \frac{a^2C_f + b^2C_r}{u}\omega_r + aC_f\delta \quad (16)$$

In this context, η and ζ are the control variables of the Sliding Mode Controller and are both positive.

2.2. EHB Braking System

Unlike traditional hydraulic brakes, there is no mechanical relationship between the brake pedal and master cylinder to generate pressure from the electro-hydraulic brake system. In addition, the braking pressure desired by the driver is sent electronically. When the brakes are installed, a measuring sensor correctly assesses its position and applies the appropriate electronic reaction to the actuator to ensure effective braking performance.

2.3. Calculation of Desired Pressure

In fig. 1, two parallel pathways are utilized to evaluate distinct pressure signals stemming from the steering angle and the driver's pedal input. Consequently, the desired pressure, P_d, is determined in two ways. The first method occurs when the driver actuates the pedal, referred to as Desired Braking Pressure (P_{db}). The second method is through the car's stability control system, which calculates the pressure proportionally to the required torque needed to compensate for the vehicle's deviation from the driver's intended steering input, known as Desired Correction Pressure (P_{dc}).

In the first mode, the desired pressure is defined as a coefficient based on the driver's pedal movement (x) relative to the maximum achievable actuator pressure (P_{max}). In the second mode, the corrective yaw moment is initially converted into the desired force. This is followed by the calculation of the force-to-pressure coefficient,c_p, which relates the longitudinal forces demanded by the stability control system (F_d) to the desired pressure. In the following equation, A_p, represents the brake piston area, and μ denotes the brake piston friction [34].

$$P_{db} = P_{max} . (x) \quad (17)$$

$$P_{dc} = {}^{F_d}/_{c_p} \quad ; \quad c_p = A_p\mu \quad (18)$$

2.4. Fuzzy Controller Design

Achieving the desired brake pressure during emergency braking is crucial to minimize vehicle speed, while effective management of deviations is essential to maintain vehicle stability, both of which are key control objectives. These objectives require careful balancing, especially when emergency braking is combined with the need for corrective braking to correct lateral yaw. During emergency braking, it is necessary to apply pressure to all wheels simultaneously, while stability control, guided by the differential braking algorithm, selectively applies pressure to specific wheels. Therefore, it is essential to balance these pressures. To navigate this complexity, a fuzzy controller optimized through genetic algorithm is implemented that allows for an effective compromise between the driver's emergency braking and the vehicle's dynamic response to deviations.

This part of the control system operates only when there is both Emergency braking and when the ESC system has detected a deviation in the vehicle and has become activated. In this case, the fuzzy controller will have two inputs based on the desired pressures to be applied to the wheels: one is the driver's braking pressure (P_{db}) and the other is the corrective pressure for the vehicle's deviation (P_{dc}). Additionally, the fuzzy control system calculates the final output based on the intensity of these computed pressures, using the defined range for membership functions and the rules derived from the linear combination of these inputs. This output indicates the priority and order of applying the computed pressures at any given moment. Thus, at any moment, an output is activated depending on the priority in relation to the applied inputs. As a result, the output oscillates between braking and reducing the vehicle's speed and applying pressure to all wheels and applying pressure to the wheels based on the algorithm in fig.7 until the conditions for the simultaneous activation of both the Emergency braking and stability control inputs are resolved.

[DOI: 10.22068/ase.2025.708]

The proposed control system in this section is the Takagi-Sugeno fuzzy controller. The inputs to the fuzzy control system are braking pressure, P_{db}, and corrective pressure, P_{dc}. Each input has five triangular membership functions corresponding to Very Low (*VL*), Low (*L*), Medium (*M*), High (*H*), and Very High (*VH*) values, as illustrated in fig. 3. Each rule is formed from the linear combination of inputs, resulting in the output of the fuzzy control system expressed as $P_{desired}$ through the weighted average method.

To determine the coefficients in the rules (75 free parameters) and identify the appropriate locations for the membership functions (30 free parameters), an optimization algorithm based on a genetic algorithm has been employed. Given the number of free parameters in the genetic structure, we have a chromosome with 105 genes representing our variables, and the number of generations is set to 100. The specifications of the GA are set according to Table1. The optimized membership functions are displayed in fig. 4.

This algorithm is designed to optimize cost function by minimizing vehicle speed and yaw rate, with respecting constraints.

$$f = \sum (K_v . V_x^{\,2} + K_e . e^2) \qquad (19)$$

where *f* represents the cost function, V_x denotes the vehicle speed and *e* signifies the disparity between the actual and desired values of yaw rate. In this paper, normalized values in the cost function have been used, with K_v set to 0.7 and K_e set to 0.3.

One key constraint limits the corrective torque or pressure, and another ensures that the total pressure at each wheel does not exceed the maximum pressure generated by the master cylinder. Additionally, maintaining the order and structure of the membership functions is essential throughout the process. This offline optimization process involves running a genetic algorithm and using a simulated model in MATLAB to determine the free parameters. Once optimized, the fuzzy control system is integrated into the main control system.

Table 1. Specifications of the GA

Genetic Parameter	Value
Population size	100
Number of Generations	150
Mutation Rate	0.01
Crossover Rate	0.8
Population type	Bit String

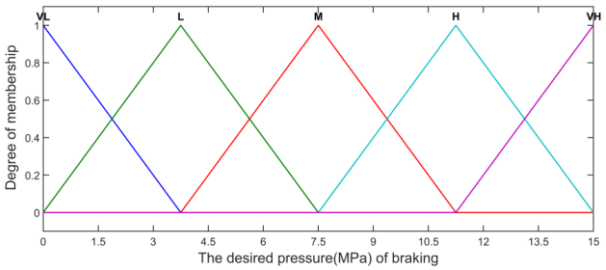

(a)

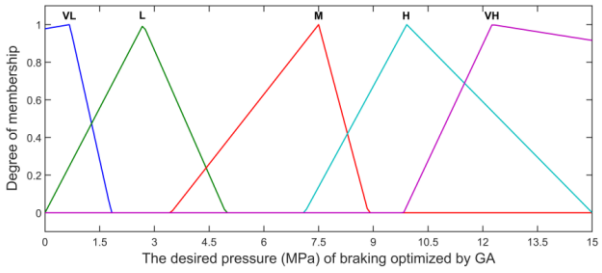

(b)

Figure 3. Membership functions of desired braking pressure (MPa): (a) before optimization (b) after optimization

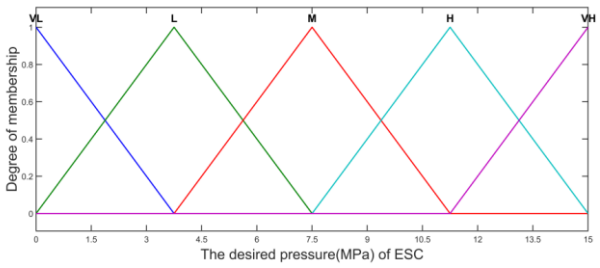

(a)

[DOI: 10.22068/ase.2025.708]

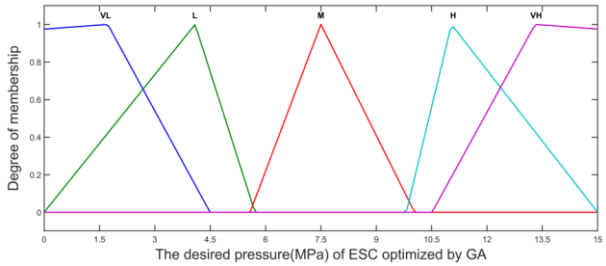

(b)

Figure 4. Membership functions of desired ESC pressure (MPa): (a) before optimization (b) after optimization

2.5. EHB Controller

To determine the motor position required to generate brake pressure in the EHB system, effective pressure control and position control are essential. As illustrated in fig. 5, a double closed-loop controller with a cascaded structure is employed to regulate the position of the PMSM motor based on the required pressure at the wheels. This configuration consists of an external loop for controlling the pressure of the master cylinder and an internal loop for managing the position of the rack.

The objective of this cascaded dual-loop controller is to manage external pressure by generating a signal for the desired position, x_{ref}, specifically tailored for the inner controller [36].

In the outer pressure loop, an x_{ref} virtual control is implemented to serve as the command input for the inner position control loop. This configuration allows the internal state bandwidth to respond faster than the external pressure loop, providing advantages in promptly addressing disturbances caused by nonlinearity and inherent uncertainties in the system. The friction force of the system is considered as just the viscous friction force. The static friction and Coulomb friction is disregarded, which is regarded as disturbance and compensated by controller .It is assumed that there is no friction loss in the pipes, elbows, valves, and other joints [36], [37].

1.1.2 Pressure Control

By defining the pressure tracking error as $\tilde{p} = p - p_d$,the error dynamics can be defined as follows [36]:

$$\dot{\tilde{p}} = \dot{p} - \dot{p}_d \tag{20}$$

By substituting (22) in the above relation, we can get

$$\dot{\tilde{p}} = \frac{A_{MC}\beta}{V_{mc} + V_{wc} - A_{MC}x}\dot{x} - \dot{p}_d \tag{21}$$

In this research, to According to author's previous study [34], the relationship between pressure and position is modeled by a simple second-order polynomial as follows:

$$p = 0.381x^2 \tag{22}$$

By calculating the time derivative of p, we can get

$$\dot{p} = 2 * 0.381x\dot{x} \tag{23}$$

This way, the sliding surface is defined.

$$s = \tilde{p} + k_0\sigma = p - p_\sigma \tag{24}$$

$$\dot{\sigma} = -k_0\sigma + \varepsilon sat\left(\frac{s}{\varepsilon}\right), \quad |\sigma(0)| \le \frac{\varepsilon}{k_0} \tag{25}$$

The time derivative s can be obtained as follows by inserting it into the above equation:

$$\begin{aligned}\dot{s} &= \dot{\tilde{p}} + k_0\dot{\sigma} \\ &= a_1\dot{p}x + a_2\dot{p} - \dot{p}_d + k_0\dot{\sigma}\end{aligned} \tag{26}$$

So x_d controller for x is designed as follows:

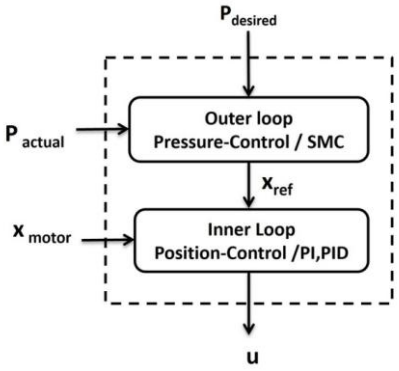

Figure 5. Double Closed-Loop Cascade Control

[DOI: 10.22068/ase.2025.708]

$$x_d = \frac{1}{a_1 \dot{p}}\left[\dot{p}_d - a_2 \dot{p} - k_0 \dot{\sigma} - c_1 s - c_2 \mathrm{sat}\left(\frac{s}{\varepsilon}\right)\right] \quad (27)$$

where in $a_1 < 0$, $a_2 > 0$

In which c_1 and c_2 are both constant and in this paper c_1=c_2=4.5e^{-4} [36].

1.1.3 Position control

This paper uses dual-layer control architecture for a Permanent Magnet Synchronous Motor (PMSM) that utilizes a three-phase inverter. The inner loop is governed by two proportional-integral (PI) controllers responsible for current regulation, while the outer loop employs two proportional-integral-derivative (PID) controllers for managing speed and position.

The output of the position controller serves as the reference for the speed controller, with the speed controller's output acting as the reference for the q-axis current controller. The d-axis current reference is maintained at zero. The system measures the position and currents of the PMSM. Velocity is obtained by taking the derivative of the position data. The PID controller outputs are produced on the dq-axis and then applied to the three-phase PMSM through inverse park conversion [38].

The output of the EHB controller is the desired pressure generated by the pressure control system via the master cylinder. This pressure is then applied to the wheels according to a specified distribution algorithm, which will be elaborated upon in the next section. Furthermore, we will demonstrate in the following section how an ABS brake system controller manages wheel slip and prevents wheel locking by adjusting the applied pressure.

2.6. Distribution Algorithm

When the driver applies the brakes while the ESC system is inactive, the braking pressure generated by the master cylinder in the EHB system is uniformly distributed across all four wheels. Conversely, when the ESC system is active, the braking pressure is allocated to the wheel that is deemed most effective based on the vehicle's current dynamics. This allocation is facilitated by a distribution algorithm that utilizes the corrective torque, denoted as M_c, as informed by the control law referenced in equation (16).The overall deviation torque resulting from the brake forces exerted on all wheels is represented by M_p, as illustrated in fig. 6 [27].

$$M_p = [(F_{fR} + F_{rR}) - (F_{fL} + F_{rL})]\frac{T_w}{2} \quad (28)$$

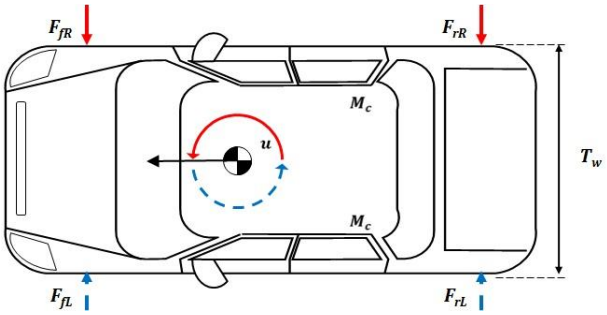

Figure 6. The lateral forces of the wheels

Note that the index ij represents the position of each tire (fL = front left, rL = rear left, fR = front right, and rR = rear right) as shown in fig. 6. In this algorithm, when the moment of corrective, M_c, equals zero (M_c=0), the forces exerted on the wheels are also zero ($F_{ij} = 0$). Conversely, in scenarios where M_c is non-zero, the brake pressure must be adjusted according to the sign of M_c, as illustrated in fig. 7. Specifically, the brake pressure on the wheels on one side should be minimized or maintained at zero, while the pressure on the opposite side should be increased to mitigate the resultant deviating torque. The associated pressure distribution algorithm is detailed in fig. 7.

It is important to identify that excessive braking force can give rise to wheel lock, an event managed by ABS, which controls the slip ratio of each wheel to prevent this phenomenon. The effective friction coefficient between the tire and the road has an optimal value that varies with road conditions; most manufacturers use a slip ratio set point, λ, of around 0.2, which serves as a good compromise for various road conditions [39],[40].

[DOI: 10.22068/ase.2025.708]

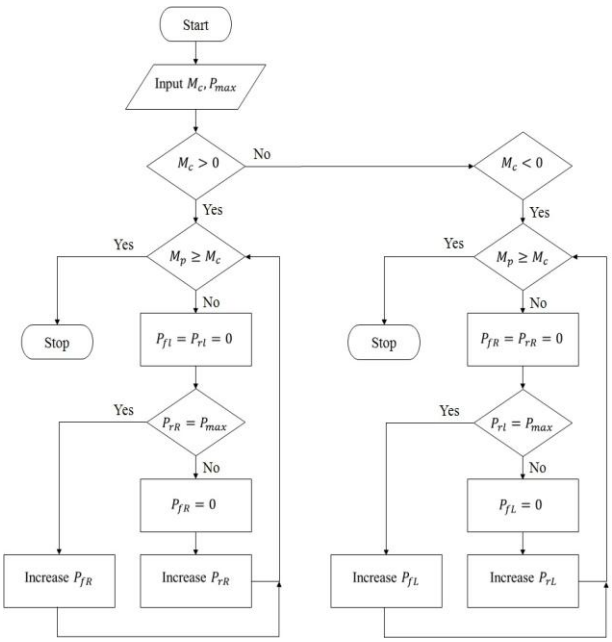

Figure 7. Pressure distribution algorithm

3. Simulation Result and Analysis

To closely replicate real vehicle dynamics, the CARSIM [41] model has been employed, providing precise, detailed, and efficient methods for simulating passenger vehicle performance. This approach includes MATLAB simulations of the EHB system along with other integrated control systems. Additionally, MATLAB is used to simulate the PMSM, implement the master cylinder system, and model the caliper-wheel components. The mechanical aspects of the EHB braking system are also simulated in MATLAB [42], with dimensions configured to resemble real-world models. Vehicle parameters are set according to Table2. The communication between the MATLAB system and CARSIM is illustrated in fig. 1.

As discussed in Section 2, there are two methods for applying pressure to the wheels: one based on the driver's pedal input and the other on the required torque to maintain vehicle stability. To enhance stability through differential braking and optimize pressure application, especially when inputs are derived from both the driver and the ESC system, a fuzzy controller optimized with a genetic algorithm is employed. This methodology aims to minimize deviation and stopping time, with pressure distribution to each wheel determined by the algorithm depicted in fig. 7. It is assumed that wheel pressure is determined via sensor measurements.

Table 2. Parameters of the case study vehicle [28]

Parameter	value	Description
m	**1231** kg	Vehicle total mass
m_s	**1111** kg	Vehicle sprung mass
l	**2.6** m	Longitudinal wheel base
a	**1.04** m	Distance of c.g. from front axle
b	**1.56** m	Distance of c.g. from rear axle
I_z	**2031.4** kg.m^2	Yaw inertia of the vehicle
R	**0.3** m	Tire radius
h_{cg}	**0.54** m	Height of c.g. of the vehicle
T_w	**1.33** m	Vehicle body width

To illustrate the impact of these two inputs, we will analyze three scenarios that clarify the interaction between driver input and vehicle mechanical deviation, thereby providing a comprehensive understanding of wheel pressure dynamics.

Scenario 1: Only the Emergency Braking is activated

To conduct more comprehensive tests, we initially assess the electro-hydraulic brake control system under stable conditions without activating the vehicle's stability control system. In this scenario, emergency braking by the driver applies appropriate pressure to the wheels based on pedal travel, measured by the position sensor x. The driver's pedal press is simulated using a ramp input, as shown in fig. 8, which applies a stroke from 0 to 30 *mm* within one second. The motor accurately follows this trajectory, transmitting a

[DOI: 10.22068/ase.2025.708]

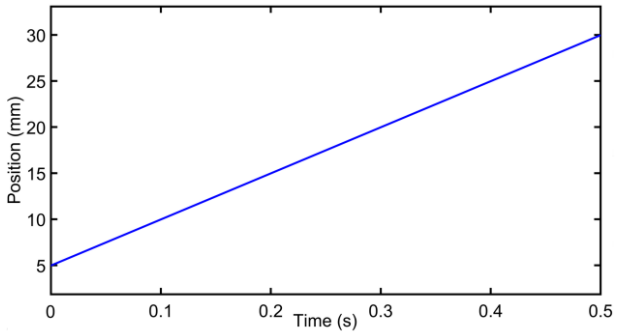

Figure 8. Brake pedal displacement

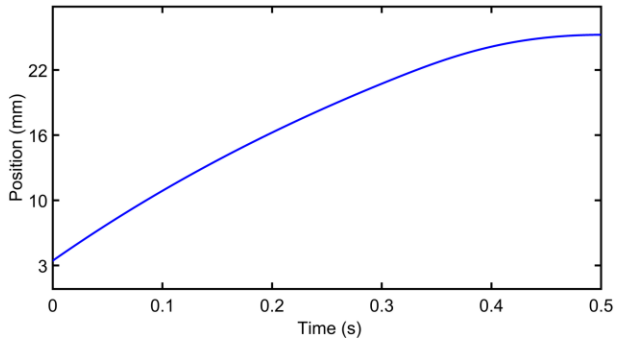

Figure 9. Displacement of the master cylinder shaft by the motor

corresponding stroke to the master cylinder shaft and thereby activating the brakes (refer to fig. 9).

The stroke applied in the master cylinder generates pressure on the wheels. Given that the maximum stroke of the master cylinder is set to 30 *mm* and the master cylinder's piston area is approximately 23 mm^2, the maximum pressure applied reaches around 10 *MPa*, peaking at 1.6 seconds. This pressure is almost equally distributed between the two front wheels and the two rear wheels. fig. 10(a) shows the controlled pressure applied to the wheels through the ramp input, while fig. 10(b) provides a clearer view of these pressures.

Scenario 2: Only the ESC is Activated

In this test, we assess the ESC system, aiming to achieve the desired yaw rate that is essential for effective steering maneuvers. To evaluate the effectiveness of the proposed control system, we conduct steering tests. During these tests, the steering angle is adjusted in a 300-degree in step mode, and the vehicle speed is set to 80 km/h. When the ESC system is activated, the wheel pressure is modified accordingly, as illustrated in fig. 11. This figure demonstrates the wheels pressure distribution based on the algorithm outlined in fig. 7 when $M_c > 0$.

Figure 13 illustrates the wheel pressure levels required to maintain stability during fishhook steering maneuvers like fig.12 and in this test the vehicle speed is set to 80 km/h. In this scenario, M_c exists in both positive and negative forms, and the pressure application algorithm corresponds to fig. 7.

According to fig.13, to ensure the vehicle's stability according to the algorithm, braking and pressurization are alternately applied to the two wheels on one side of the car based on the sign of M_c.

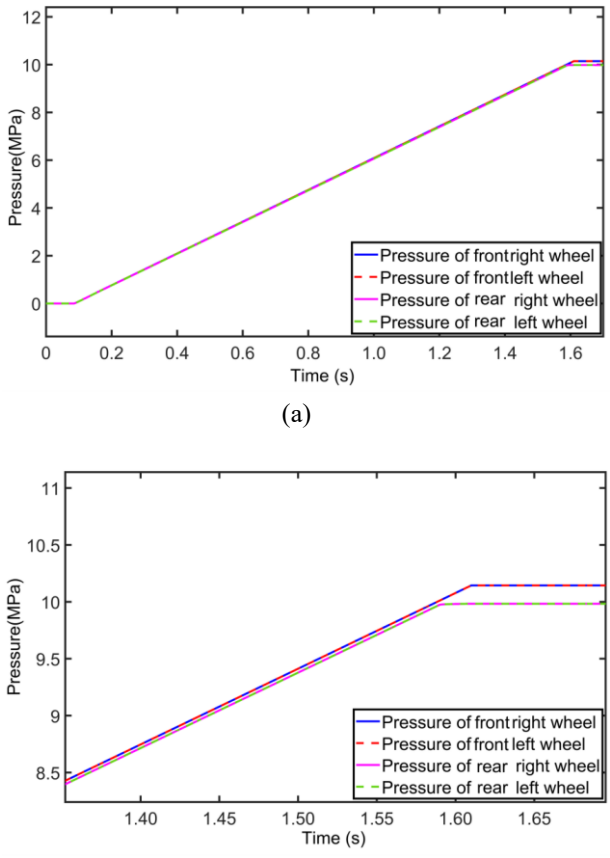

Figure 10. The pressure applied to the wheels by the ramp input

[DOI: 10.22068/ase.2025.708]

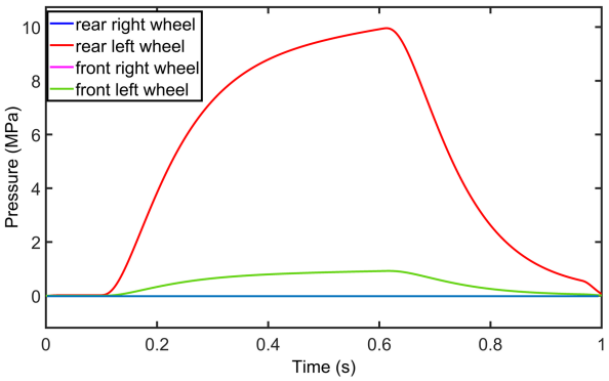

Figure 11. The pressure applied to the wheels according to the algorithm

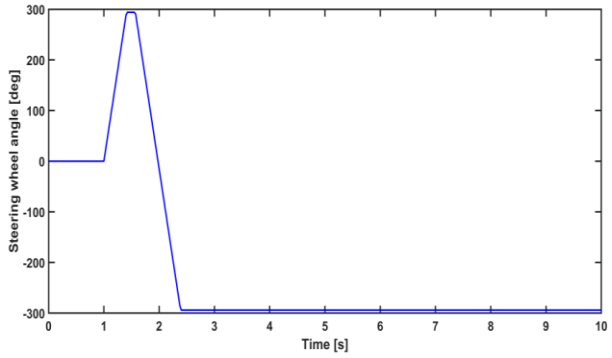

Figure 12. Fishhook steering test

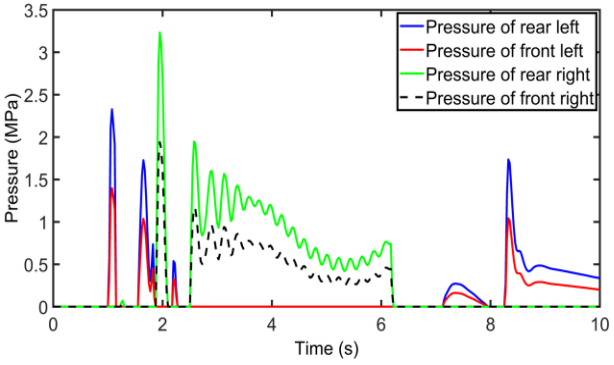

Figure 13. Pressure on each wheel in fishhook steering test

Scenario 3: Both the ESC system and the EB are Activated together

One of the main challenges of this research is to apply optimal pressure on the wheels when the driver engages the brakes while simultaneously controlling the vehicle's stability in corners. To address this, we conduct a braking test initiated by the driver alongside a steering maneuver. In this scenario, both the driver's braking input and the correction of the vehicle's deviation are activated simultaneously.

As mentioned previously, an optimized fuzzy control system utilizing a genetic algorithm is responsible for balancing these two types of braking. The primary objectives of this optimized fuzzy control system are to reduce speed, minimize the vehicle's deviation from the desired state, and to prioritize the application of appropriate pressures.

Figure 14(a) depicts a test involving a fishhook steering angle maneuvers like Fig.12 and in this test the vehicle speed is set to 80 km/h., where the driver quickly presses the brake pedal (Pedaling speed above 7 mm/s). This test demonstrated that during emergency braking, the ESC is also activated at the appropriate time and maintains the stability of the vehicle by applying appropriate pressures.

Simulation results show that the proposed control system not only enhances stability, but also ensures that the vehicle speed is reduced without deviation in a short time.

As illustrated in fig. 14(a) and more clearly in fig. 14(b), the activation of the stability control system in response to the car's fishhook movement results in pressure being applied to the wheels on one side of the vehicle according to the algorithm presented in fig. 7, while the pressure on the wheels on the opposite side drops to zero.

In fig. 14(b), at 6.75 seconds, the driver initiates braking, which prompts an immediate response where pressure is applied to all four wheels, with the pressures illustrated as superimposed in the figure. For a brief period, the ESC system remains inactive due to the vehicle's low speed. Around 2.9 seconds, the ESC system applies a small amount of pressure to the left wheels.

For instance, in fig. 14(c), at 1.55 seconds, pressure is applied to the left wheels, starting with the left rear wheel, followed by a lesser degree of pressure on the left front wheel. At approximately 1.87 seconds, as dictated by the algorithm in fig. 7,

[DOI: 10.22068/ase.2025.708]

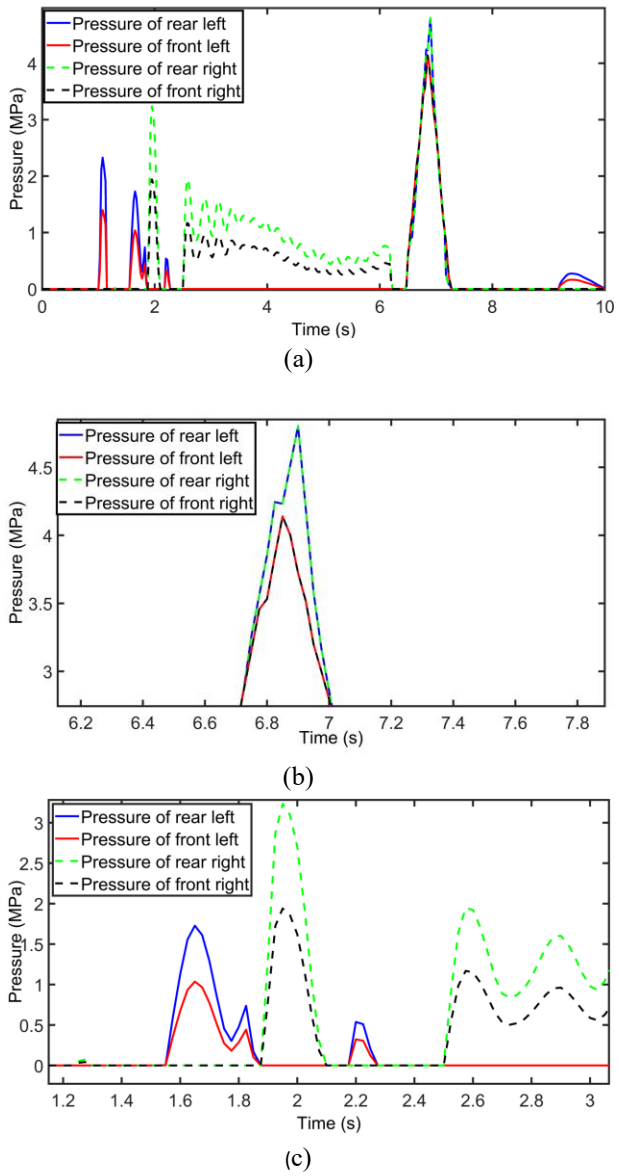

Figure 14. Pressure on each wheel in fishhook steering test with braking

pressure is then applied to the right wheels, causing the pressure on the left wheels to drop to zero.

In fig.15, the yaw rate diagram is analyzed for the three previously mentioned scenarios:

a. When vehicle stability has a higher priority.
b. When emergency response to braking has a higher priority.
c. When the fuzzy control system determines the priority, which is the focus of this study.

If the emergency braking occurs between 6 and 7 seconds and the steering angle follows fig. 12, the yaw rate for the above three cases will be as shown in fig.15. The best stability control is achieved when ESC control has a higher priority, while the worst yaw rate occurs when the driver's braking response has a priority.

Figure 16 examines the vehicle speed and shows that the largest speed reduction occurs when the driver's braking has a priority. Based on the results in figures 15 and 16, to achieve a balance between these two critical challenges, it can be beneficial to use an auxiliary controller to determine the response priority.

Comparison of the above three scenarios in figures 15 and 16 shows that the proposed method, (fuzzy system determines the priority), in addition to performing stability control well to reduce yaw rate, also has a good speed reduction during emergency braking in corners.

At the critical point of 8.3 seconds, the analysis shows that the fuzzy-GA controller reduced yaw rate overshoot by around 16% compared to ESC-priority mode while maintaining an around 60% of the deceleration performance of EB-priority mode.

To evaluate the performance of the proposed method, the obtained results were compared with

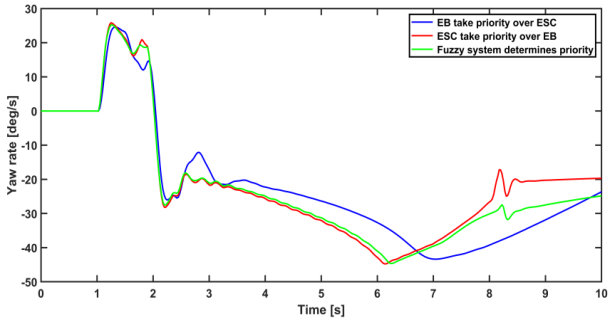

Figure 15. Yaw rate in fishhook steering test

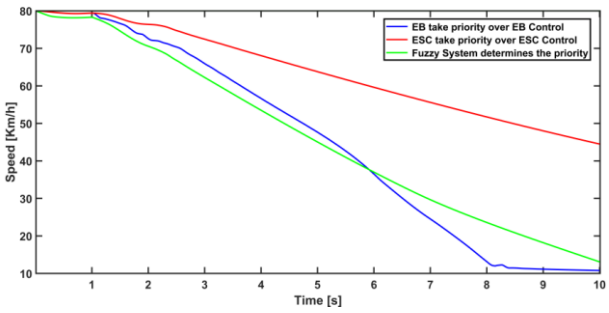

Figure 16. Vehicle speed in fishhook steering test

[DOI: 10.22068/ase.2025.708]

those presented in the benchmark paper [43]. In the mentioned study, MPC-based ESC was used for stability control of vehicle. By comparing the yaw rate with the that paper, it is observed that due to the smaller steering angle (200 deg) compared to the steering angle in proposed paper, the yaw rate has significantly improved.

4. Conclusion

The use of the differential brake system to control vehicle stability has challenges, especially when the stability control system is automatically activated simultaneously with driver emergency braking. In such scenarios, it is essential to maintain vehicle stability and minimize vehicle speed to an ideal level. Recently, the EHB has replaced the traditional vacuum brake booster and offers significant benefits in pressure control and maximum pressure production capacity. In addition, an ABS is required to prevent the wheels from blocking the wheels due to excessive pressure. This paper presents an integrated system that effectively addresses these challenges.

The structure described in this paper includes an EHB controller that enables rapid pressure increase and precise wheel pressure control. In addition, the proposed parallel architecture for simultaneous stability and brake control ensures that optimal pressure is applied to the wheels during emergency braking in corners. This allows for timely deceleration while maintaining vehicle stability. Furthermore, when integrated with the ABS system, it prevents wheel locking, which helps maintain longitudinal slip of the vehicle.

In addition, this paper introduces a novel control architecture that balances the braking control, especially during emergency braking, to reduce the speed while maintaining vehicle stability. The results show that the proposed control structure not only effectively maintains vehicle stability, but also provides a responsive performance during emergency braking, allowing the vehicle to decelerate in the shortest possible time in corners.

In this paper, the feasibility of simultaneous control ESC and Emergency braking for vehicle stability control and rapid speed reduction in emergency situations is explore in theory. The proposed method is verified in software-in-loop (SIL) test, which is different with hardware-in-loop (HIL) and real driving experiment, e.g., signal disturb or delay. To this end, the proposed method will implement in HIL platform and a prototype vehicle in the future. also, it's recommended to integration with active steering.

References

[1] He, X., Yang, K., Ji, X., Liu, Y. et al., "Research on Vehicle Stability Control Strategy Based on Integrated-Electro-Hydraulic Brake System," SAE Technical Paper 2017-01-1565, 2017, doi: https://doi.org/10.4271/2017-01-1565.

[2] M. M. Tehrani, et al.," Design of an Anti-Lock Regenerative Braking System for a Series Hybrid Electric Vehicle", International Journal of Automotive Engineering, Vol. 1, Number 2, June 2011, doi: 10.4271/2018-01-0816.

[3] M. Ajami1, H. Jannat, M. Masih- Tehrani, " The Effect of Tire Pressure Changes on Braking Efficiency and Necessity of Adjusting Tire Pressure Before Braking Test at Vehicle Technical Inspection Centers", Automotive Science and Engineering, Vol. 10, No. 4, (2020), 3446-3456, doi: 10.22068/ijae.10.4.3446.

[4] Kumar, D.K. and T.R.D. Gaddam, "Fuzzy logic controller based performance of SPMSM fed with improved direct torque control", International Journal of Renewable Energy Research (IJRER), 2019. 9(3): p. 1346-1354, doi: 10.20508/ijrer.v9i3.9625.g7714,

[5] Bida, V.M., D.V. Samokhvalov, and F.S. Al-Mahturi, " PMSM vector control techniques—A survey", in 2018 IEEE Conference of Russian Young Researchers in Electrical and Electronic Engineering (EIConRus). 2018. IEEE, doi:10. 1109/EIConRus.2018.8317164.

[6] Li, S., et al., "Neural-network vector controller for permanent-magnet synchronous motor drives: Simulated and hardware-validated results", IEEE transactions on cybernetics, 2019. 50(7): p. 3218-3230, doi: 10.1109/TCYB.2019.2897653.

[7] Wang, X., Z. Wang, and Z. Xu, "A hybrid direct torque control scheme for dual three-phase PMSM drives with improved operation performance", IEEE Transactions on Power Electronics, 2018. 34(2): p. 1622-1634, doi:10.1109/TPEL.2018.2835454.

[8] Mynar, Z., L. Vesely, and P. Vaclavek, "PMSM model predictive control with field-weakening implementation", IEEE Transactions on Industrial Electronics, 2016.

[DOI: 10.22068/ase.2025.708]

63(8): p. 5156-5166, doi: 10.1109/TIE.2016.2558165.
[9] Younesi, A., S. Tohidi, and M. Feyzi, "Improved optimization process for nonlinear model predictive control of PMSM", Iranian Journal of Electrical & Electronic Engineering, 2018. 14(3): p. 278, doi:10.22068/IJEEE.14.3.278.
[10] Luo, Y. and C. Liu," A simplified model predictive control for a dual three-phase PMSM with reduced harmonic currents", IEEE Transactions on Industrial Electronics, 2018, 65(11): p. 9079-9089, doi: 10.1109/TIE.2018.2814013.
[11] Mendoza-Mondragón, F., V.M. Hernández-Guzmán, and J. Rodríguez-Reséndiz, "Robust speed control of permanent magnet synchronous motors using two-degrees-of-freedom control", IEEE Transactions on Industrial Electronics, 2018. 65(8): p. 6099-6108, doi: 10.1109/TIE.2017.2786203.
[12] Zhao, Y. and L. Dong, "Robust current and speed control of a permanent magnet synchronous motor using SMC and ADRC", Control Theory and Technology, 2019. 17: p. 190-199, doi: 10.1007/s11768-019-8084-y.
[13] Mo, L., Y. Liu, and Y. Zhang, "Sliding mode variable structure control for surface permanent magnet synchronous motors based on a fuzzy exponential reaching law",Mathematical Problems in Engineering, 2019. 2019, doi: 10.1109/ACCESS.2019.2946349.
[14] Xu, W., et al., "Improved continuous fast terminal sliding mode control with extended state observer for speed regulation of PMSM drive system", IEEE Transactions on Vehicular Technology, 2019, 68(11): p. 10465-10476, doi: 10.1109/TVT.2019.2926316.
[15] Chen, P., et al., "Design and position control of a novel electric brake booster", SAE International Journal of Passenger Cars-Mechanical Systems, 2018. 11(2018-01-0812): p. 389-400, doi: 10.4271/2018-01-0812.
[16] Zhang, H., et al., "Development and Verification of Control Algorithm for Permanent Magnet Synchronous Motor of the Electro-Mechanical Brake Booster", 2019, SAE Technical Paper, doi: 10.4271/2019-01-1105.
[17] Chen, P., et al., "Design and Power-Assisted Braking Control of a Novel Electromechanical Brake Booster", SAE International Journal of Passenger Cars-Electronic and Electrical Systems, 2018. 11(2018-01-0762): p. 171-181, doi: 10.4271/2018-01-0762.
[18] Han, W., L. Xiong, and Z. Yu, "Braking pressure control in electro-hydraulic brake system based on pressure estimation with nonlinearities and uncertainties", Mechanical Systems and Signal Processing, 2019. 131: p. 703-727, doi: 10.1016/j.ymssp.2019.02.009.
[19] Ji, Y., et al., "Constraint performance pressure tracking control with asymmetric continuous friction compensation for booster based brake-by-wire system", Mechanical Systems and Signal Processing, 2022. 174: p. 109083, doi: 10.1016/j.ymssp.2022.109083.
[20] Chen, Q., et al., "Hydraulic-pressure-following control of an electronic hydraulic brake system based on a fuzzy proportional and integral controller", Engineering Applications of Computational Fluid Mechanics, 2020. 14(1): p. 1228-1236, doi: 10.1080/19942060.2020.1816495.
[21] Soliman, A.M., et al., "Vehicle Braking Performance Improvement via Electronic Brake Booster", SAE International Journal of Vehicle Dynamics, Stability, and NVH, 2024. 8(10-08-01-0005), doi: https://doi.org/10.4271/10-08-01-0005.
[22] Gao, Z., et al., "Adaptive Pressure Estimation and Control Architecture for Integrated Electro-Hydraulic Brake System", 2022, doi: 10.21203/rs.3.rs-1793406/v1.
[23] Wei, H., L. Xiong, and Z. Yu, "Braking pressure tracking control of a pressure sensor unequipped electro-hydraulic booster based on a nonlinear observer", 2018, SAE Technical Paper, doi: https://doi.org/10.4271/2018-01-0581.
[24] Lao, D., et al., "Research on Yaw Stability Control of Unmanned Vehicle Based on Integrated Electromechanical Brake Booster", 2020, SAE Technical Paper, doi: https://doi.org/10.4271/2020-01-0212.
[25] Shayan Nazemi, Masoud Masih-Tehrani and Morteza Mollajafari, " GA tuned H∞ roll acceleration controller based on series active variable geometry suspension on rough roads", Int. J. Vehicle Performance, Vol. 8, Nos. 2/3, 2022, doi: 10.1504/IJVP.2022.122047.
[26] Andras Bartfai, Illes Voros and Denes Takacs, " Stability analysis of a digital hierarchical steering controller of autonomous vehicles with multiple time delays",Journal of Vibration and Control ,2023, Vol. 0(0) 1–12, doi: 10.1177/09544070231217558.
[27] Mirzaeinejad, H., M. Mirzaei, and S. Rafatnia, "A novel technique for optimal integration of active steering and differential braking with estimation to improve vehicle directional stability", ISA transactions, 2018. 80: p. 513-527, doi: 10.1016/j.isatra.2018.05.019.
[28] Chen, Z., Y. Wu, and F. Li, "Integrated control of differential braking and active aerodynamic control for improving high speed stability of vehicles", International Journal of Automotive Technology, 2020, 21: p. 61-70, doi: 10.1007/s12239-020-0007-x.

[DOI: 10.22068/ase.2025.708]

[29] Hamid Gheibollahi, Masoud Masih-Tehrani, Amin Najafi, " Improving ride comfort approach by fuzzy and genetic-based PID controller in active seat suspension", Int. J. Automation and Control, Vol. 18, No. 2, 2024, doi: 10.3390/en13236183.

[30] Amin Najafi · Masoud Masih‑Tehrani and et al., " A modern multidimensional fuzzy sliding mode controller for a series active variable geometry suspension", Journal of the Brazilian Society of Mechanical Sciences and Engineering (2022) 44: 425, doi: 10.1007/s40430-022-03735-0.

[31] Hossein Nazemian ,Masoud Masih-Tehrani, " Hybrid Fuzzy-PID Control Development for a Truck Air Suspension System", SAE Int. J. Commer. Veh. / Volume 13, Issue 1, 2020, doi: 10.4271/02-13-01-0004.

[32] Huang, Z. and Y. Wu, "Lane departure Assistance based on balanced longitudinal slip ratio differential braking control", International Journal of Vehicle Safety, 2015. 8(3): p. 205-217, doi: 10.1504/IJVS.2015.070767.

[33] Rajamani, R. and R. Rajamani, Electronic stability control. Vehicle Dynamics and Control, 2012: p. 201-240, doi: 10.1007/978-1-4614-1433-9_8.

[34] Montani, M., et al., "Performance review of three car integrated abs types: development of a tire independent wheel speed control". Energies, 2020. 13(23): p. 6183, doi: 10.3390/en13236183.

[35] Han, W., L. Xiong, and Z. Yu, "A novel pressure control strategy of an electro-hydraulic brake system via fusion of control signals", Proceedings of the Institution of Mechanical Engineers, Part D: Journal of Automobile Engineering, 2019. 233(13): p. 3342-3357, doi: 10.1177/0954407018821016.

[36] Han, W., L. Xiong, and Z. Yu, "Interconnected pressure estimation and double closed-loop cascade control for an integrated electro hydraulic brake system", IEEE/ASME Transactions On Mechatronics, 2020. 25(5): p. 2460-2471, doi: 10.1109/TMECH.2020.2978534.

[37] Hossein Nazemian ,Masoud Masih-Tehrani, " Development of an Optimized Game Controller for Energy Saving in a Novel Interconnected Air Suspension System", Proceedings of the Institution of Mechanical Engineers Part D Journal of Automobile Engineering , April 2020, doi: 10.1177/0954407020927147.

[38] Kizir, G. and A.F. Kanburoglu, "Position Control of External Rotor Permanent Magnet Synchronous Motor with Model Predictive Control", in Model Predictive Control-Theory and Applications, 2023,IntechOpen, doi: 10.30420/566091226.

[39] Lin, C.-M. and C.-F. Hsu, "Self-learning fuzzy sliding- mode control for antilock braking systems", IEEE Transactions on Control Systems Technology, 2003. 11(2): p. 273-278, doi: 10.1109/TCST.2003.809246.

[40] Raesian, N., N. Khajehpour, and M. Yaghoobi. "A new approach in anti-lock braking system (ABS) based on adaptive neuro-fuzzy self-tuning PID controller", in The 2nd international conference on control, instrumentation and automation. 2011. IEEE, doi: 10.1109/ICCIAutom.2011.6356714.

[41] Mechanical Simulation Corporation, "CarSim", 2016 , https://www.carsim.com.

[42] MathWorks, Inc., "MATLAB" , 2020, https://www.mathworks.com.

[43] Liang Li, Yishi Lu and et al., " A Three-Dimensional Dynamics Control Framework of Vehicle Lateral Stability and Rollover Prevention via Active Braking With MPC", IEEE TRANSACTIONS ON INDUSTRIAL ELECTRONICS, VOL. 64, NO. 4, APRIL 2017, doi: 10.1109/TIE.2016.2583400.

[DOI: 10.22068/ase.2025.708]